Bi-rich, and Sr- and Ca-poor (*2*). Extra Bi atoms may occupy Sr or Ca sites to compensate for the Bi vacancies in the BiO planes. Rutherford backscattering and microprobe analyses of these particular crystals suggested that they were slightly Bi-rich, but the spread in the data makes such measurements inconclusive.

In conclusion, an STM operating in UHV conditions has been used to resolve the atomic structure of the BiO surface plane of single-crystal $Bi_2Sr_2CaCu_2O_{8+\delta}$. Missing rows of Bi atoms and a displacive modulation of the Bi atoms both parallel and perpendicular to the *a-b* plane are responsible for the superstructure seen in this compound. The missing rows occur on every ninth or tenth lattice site, yielding an average spacing that agrees with the incommensurate perodicity seen in TEM and x-ray data of the bulk crystal structure. The lateral displacive modulation measured by STM has the same amplitude and phase (relative to the phase of the vertical buckling modulation) as those seen by x-ray measurements of the bulk. Thus, the structure of the surface BiO plane corresponds to that of the bulk BiO planes. Because the double BiO layers in the bulk are weakly held together, the surface reconstruction of the BiO plane is expected to be small. X-ray data has shown that the Cu atoms in the (2:2:1:2) crystal are buckled, perturbing the electronic states of the CuO plane. Other superstructures have been recently measured in the related Tl containing compounds (*16*). Therefore, the superstructure studied in the (2:2:1:2) compound may not just be an oddity of this complicated crystal structure. In fact, such superlattice behavior may critically affect the superconducting properties of this class of cuprate superconductors.

REFERENCES AND NOTES

1. M. A. Subramanian *et al.*, *Science* **239**, 1015 (1988).
2. S. A. Sunshine *et al.*, *Phys. Rev. B* **38**, 893 (1988).
3. T. M. Shaw *et al.*, *ibid.* **37**, 9856 (1988).
4. J. M. Tarascon *et al.*, *ibid.*, p. 9382.
5. P. A. P. Lindberg *et al.*, in preparation.
6. M. D. Kirk *et al.*, *Appl. Phys. Lett.* **52**, 2071 (1988).
7. The first atomic resolution images in air on (2:2:1:2) were taken by Virgil Elings (Digital Instruments) and were presented at the Third International STM Conference, Royal Microscopical Society, Oxford, England, 4 to 8 July 1988.
8. H. W. Zandbergen, P. Groen, G. Van Tendeloo, J. Van Landuyt, S. Amelinckx, *Solid State Commun.* **66**, 397 (1988).
9. Y. Gao, P. Lee, P. Coppens, M. A. Subramanian, A. W. Sleight, *Science* **241**, 954 (1988).
10. S. Park and C. F. Quate, *Rev. Sci. Instrum.* **58**, 2010 (1987).
11. S. L. Tang, R. V. Kasowski, M. A. Subramanian, W. Y. Hsu, *Physica C* **156**, 177 (1988).
12. M. S. Hybertsen and L. F. Mattheiss, *Phys. Rev. Lett.* **60**, 1661 (1988).
13. H. Krakauer and W. E. Pickett, *ibid.*, p. 1665.
14. F. Herman, R. V. Kasowski, W. Y. Hsu, *Physica C* **153–155**, 629 (1988).
15. P. A. P. Lindberg *et al.*, *Appl. Phys. Lett.*, in press.
16. R. Beyers *et al.*, *ibid.* **53**, 432 (1988).

17. The authors thank A. Marshall, R. Barton, and W. Harrison for useful discussions. L. LaComb assisted with image processing software. Three of the authors would like to acknowledge support received through AT&T Ph.D. Fellowships (A.A.B. and D.B.M.) and Alfred P. Sloan and P.Y.I. Fellowships (A.K.). This work was supported by the Defense Advanced Research Projects Agency, the Office of Naval Research, and by the National Science Foundation Materials Research Laboratory Program through the Center for Materials Research at Stanford University.

27 October 1988; accepted 18 November 1988

Gravitational Separation of Gases and Isotopes in Polar Ice Caps

H. CRAIG, Y. HORIBE,* T. SOWERS†

Atmospheric gases trapped in polar ice at the firn to ice transition layer are enriched in heavy isotopes (nitrogen-15 and oxygen-18) and in heavy gases (O_2/N_2 and Ar/N_2 ratios) relative to the free atmosphere. The maximum enrichments observed follow patterns predicted for gravitational equilibrium at the base of the firn layer, as calculated from the depth to the transition layer and the temperature in the firn. Gas ratios exhibit both positive and negative enrichments relative to air: the negative enrichments of heavy gases are consistent with observed artifacts of vacuum stripping of gases from fractured ice and with the relative values of molecular diameters that govern capillary transport. These two models for isotopic and elemental fractionation provide a basis for understanding the initial enrichments of carbon-13 and oxygen-18 in trapped CO_2, CH_4, and O_2 in ice cores, which must be known in order to decipher ancient atmospheric isotopic ratios.

ISOTOPIC RATIOS OF ATMOSPHERIC gases trapped in polar ice cores provide important data for understanding the atmospheric history of O_2 (*1–3*), CO_2 (*4*), and CH_4 (*5*), and the past variations in sources and sinks of these gases. Thus it is essential that fractionation mechanisms in polar firn layers that may affect the composition (isotopic and chemical) of gases before trapping in nascent ice beneath the firn be identified and understood. Horibe *et al.* (*1*) originally reported that O_2 trapped in 2000-year-old ice from Camp Century, Greenland, has an $^{18}O/^{16}O$ enrichment given by $\delta(^{18}O) = 0.61$ per mil versus present-day atmospheric O_2 (*6*). Bender *et al.* (*2*) reported essentially zero ^{18}O enrichments in O_2 in Holocene ice from the Antarctic D-10 and Dome C cores, with, however, significant enrichments in O_2 in Pleistocene ice in these cores, similar to those observed in older Greenland ice (*1*). These data therefore indicated that fractionation effects during accumulation of firn, possibly occurring only in Greenland ice, might affect the isotopic records of O_2 and other gases in ice cores.

H. Craig and Y. Horibe, Isotope Laboratory, Scripps Institution of Oceanography, University of California at San Diego, La Jolla, CA 92093.
T. Sowers, University of Rhode Island, Graduate School of Oceanography, Narragansett, RI 02882.

*Present address: School of Marine Science, Tokai University, Shizuoka, Japan 424.
†Present address: Laboratoire Glaciologie et Geophysique de l'Environnement, BP 96, 39402 Saint Martin d'Heres, Cedex, France.

In this report we show that ^{15}N and ^{18}O enrichments are present in N_2 and O_2 in Recent ice from Greenland Dye 3 ice core. One of us (*3*) has observed similar enrichments in Greenland and Antarctic ice, together with variations in major gas composition. We propose that the major fractionation process affecting these gases and isotopes is gravitational separation in the firn layer above the ice. Other effects on gas chemistry appear to reflect differential gas losses in accordance with experimental observations and expected capillary conduc-

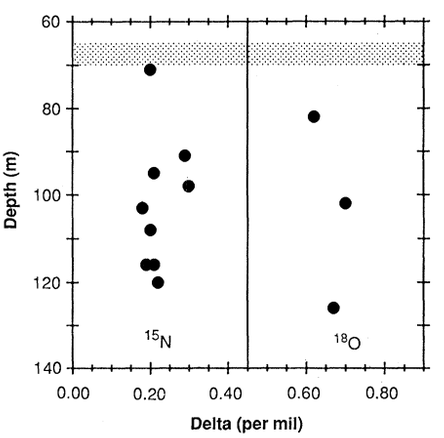

Fig. 1. Measurements of $\delta(^{15}N)$ and $\delta(^{18}O)$ relative to air in trapped N_2 and O_2 in the Dye 3 Greenland ice core, versus depth. Experimental precision is $\sim \pm 0.05$ per mil for each isotope (*6*). The firn to ice transition (stippled region) is at 65 to 70 m (*8*).

Table 1. Isotopic and component enrichment comparisons for the effusion process with F_L, the fraction of gas lost at the fractionating stage, set equal to 2%, and with $Z = 75$ m, $T = -20$°C, for the gravitational effect, thus setting the same ^{15}N enrichment for both processes.

Components	Δ(Effusion) (per mil)	Δ(Gravitational) (per mil)
$\delta(^{15}N)$	0.35	0.35
$\delta(^{18}O)$	0.60	0.70
$\Delta(O_2/N_2)$	1.30	1.40
$\Delta(Ar/N_2)$	3.30	4.20
$\Delta(Kr/N_2)$	8.6	19.6

tance rates, in the order $O_2 > Ar > N_2$.

Data measured at Scripps Institution of Oceanography (SIO) on ^{15}N and ^{18}O enrichments in N_2 and O_2 in the upper 130 m of the Greenland Dye 3 core are shown in Fig. 1 (7). In this core the transition from firn to ice is at a depth of 65 to 70 m (*8*) and the samples, beginning just below the transition zone, show that isotopic enrichments occur in the youngest ice in the core and are therefore caused by a fractionation processes in the accumulating firn. We discuss two possible processes that can account for the observed heavy isotope enrichments: (i) gravitational separation of gases in the porous firn layer and (ii) effusion from partially sintered pores above the transition layer.

The gravitational equilibrium for a perfect-gas component at depth Z in a firn layer is given by (*9*):

$$p/p^0 = \exp\,[MgZ/R^+T] \qquad (1)$$

in which M = molecular mass, g is the gravitational acceleration at ~70°N, R^+ is the gas constant, and T is absolute temperature. Here p is the partial pressure of the component in the gas-filled pores, and the zero superscript refers to the surface (atmospheric) value at each site. Thus if R is the ratio of any two components (isotopes, gases), and the per mil enrichment of R relative to the atmospheric ratio R^0 is $\Delta = 10^3 (R/R^0 - 1)$ [that is, like the isotopic enrichments (*6*)], then the enrichment of a species N_i versus a second species N, relative to the atmospheric ratio, is simply:

$$\Delta(N_i/N) = 10^3 \cdot \Delta M \cdot gZ/RT \qquad (2)$$

where we have used the approximation $\ell n(1 + x) \approx x$, and have set $\Delta M = (M_i - M)$, the mass difference in atomic mass units (AMU) between the two components. We assume that the chemical potentials are given by the partial pressures in the gas mixture. The predicted enrichment effect is then given numerically by $\Delta = (1.18/T)Z$ per mil per AMU. Thus at Dye 3 with $Z = 70$ m and $T = -20$°C (*8*), Eq. 2 predicts that $\delta(^{15}N)$ and $\delta(^{18}O)$ will be 0.33 and 0.66 per mil. Figure 1 shows that the observed mean $\delta(^{15}N)$ is 0.22 per mil, 67% of that predicted, whereas for $\delta(^{18}O)$ the observed mean, 0.65 per mil, is precisely that predicted.

There are three important points about the gravitational effect: (i) the enrichment effect is mass independent in that it depends only on the mass difference, and not, as in other processes such as effusion, on the fractional mass difference $\Delta M/M$; (ii) the maximum separation effect for two components is predicted a priori by Eq. 2 for the depth and temperature of any firn layer; no assumption as to fractional removal of gases from a part of the system is necessary; and (iii) establishment of the equilibrium concentration gradients by molecular diffusion is opposed by an upward advective flow of gas caused by compression of the firn. This flow decreases with increasing depth as the firn density approaches the final close-off value of 0.83, the value for ice sealed with about 10% by volume of occluded air in the encapsulated bubbles. Thus the observed enrichment effects in the ice layers may vary from the maximum predicted effect to zero, depending on advection (that is, accumulation) rates and mixing effects in the firn (*10*).

In Fig. 2 we show the predicted and measured ^{18}O and ^{15}N enrichments for the Dye 3 site (SIO data) and for a D-57 core from a coastal site in Terre Adelie in Antarctica [measurements made at the University of Rhode Island (URI) (*3, 7*)]. At D-57 the firn thickness $Z = 76$ m and $T = -32$°C, so that the predicted ^{15}N and ^{18}O enrichments are 0.37 and 0.75 per mil, respectively. The measured enrichments for three sets of samples (87.6-m, 90-m, and 197-m depth) are consistent (range = 0.10 per mil for N_2 and 0.15 per mil for O_2) with a slope of 2.1. The mean values are $\delta(^{15}N) = 0.34 \pm 0.04$, and $\delta(^{18}O) = 0.72 \pm 0.08$ per mil, almost precisely the predicted values. The accumulation rate of ice at the D-57 site is only 0.18 m/year, which may account for the better agreement than in the case of Dye 3, where the rate is 0.49 m/year and the advective flux is therefore considerably greater.

Figure 2 also shows two analyses for a single sample from the Antarctic Dome C core (*11*) where $Z = 78$ m, $T = -53$°C. The predicted enrichments are 0.42 per mil for ^{15}N and 0.84 per mil for ^{18}O. The observed values (*3*) are 0.41 per mil for ^{15}N, as predicted, and 1.15 per mil for ^{18}O. However, the air in this sample is 2200 years old (*3*), and Sowers *et al.* point out that the isotopic composition of atmospheric O_2 may have differed by that much at that time (that is, by 1.15 − 0.84 = only 0.31 per mil).

Other URI data (*3*) lie between the D-57 data and the atmospheric composition at the origin, all values being positive for both

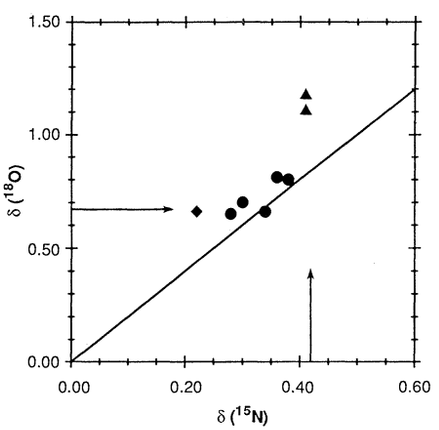

Fig. 2. Values of $\delta(^{15}N)$ and $\delta(^{18}O)$ measured on Dye 3 ice core samples (SIO data, diamond), and D-57 (dots) and Dome C (triangles) samples (*3*). The line is the calculated gravitational equilibrium relation (slope = 2). The maximum D-57 enrichments for both isotopes, the Dye 3–^{18}O enrichment (horizontal arrow), and the Dome C–^{15}N enrichment (vertical arrow) are predicted exactly from the firn depths and temperatures.

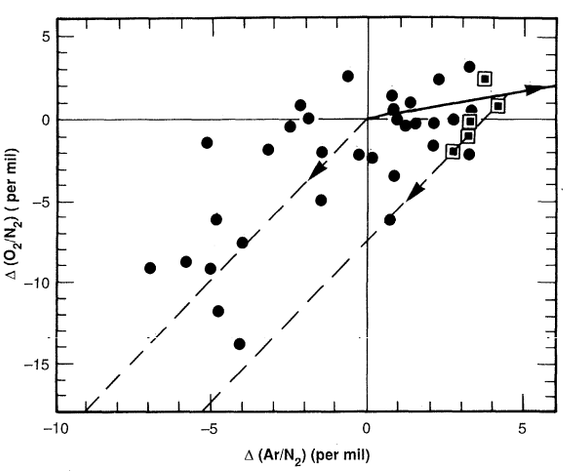

Fig. 3. Measurements of O_2/N_2 and Ar/N_2 enrichments relative to air values (*3*). Squares mark the D-57 values corresponding to data in Fig. 2. The line in the upper right quadrant (slope = 1/3) is the gravitational equilibrium vector. The lines in the lower quadrangles (negative enrichments) are the mean vector observed in nonequilibrium gas extraction by pumping on fractured ice samples, drawn from the origin and the point of maximum enrichments. The positive and negative enrichments, coupled with the positive enrichments in Fig. 2, indicate that two processes are determining the effects observed in these analyses.

isotopes, with a slope of ~2 but with a $\delta(^{18}O)$ intercept of +0.13 per mil. The intercept value may be a real age effect (*3*) or an artifact of the differential loss effects discussed below: available data are not sufficient to decide the point. Our maximum predicted values for polar ice are at the Antarctic Vostok site (78.5°S), with $Z = 96$ m and $T = -57$°C and an accumulation rate of only 0.022 m of ice per year (*8*): 0.52 and 1.04 per mil for ^{15}N and ^{18}O enrichments.

In Fig. 3 we show the general spectrum of $\Delta(O_2/N_2)$ and $\Delta(Ar/N_2)$ values measured at URI (*3*). The predicted gravitational enrichments (Eq. 2) for perfect gas mixtures and for mass differences of 4 and 12 AMU, respectively, correspond to maximum $\Delta(O_2/N_2)$ and $\Delta(Ar/N_2)$ values of 1.5 and 4.5 per mil. Figure 3 shows that these values are close to the maximum enrichments of 1.5 and 4.0 per mil found in the D-57 core, the highest values that have been observed.

A second major effect is that large negative enrichments of the O_2/N_2 and Ar/N_2 ratios are also present in some gases. That is, the data as a whole indicate that both positive and negative enrichments of the heavy-gas (O_2 and Ar) ratios to N_2 can occur, but these are always coupled with positive enrichments of the heavy isotopes ^{15}N and ^{18}O. Clearly more than one process is necessary to account for this pattern of elemental and isotopic fractionation. Experiments at SIO indicate that differential capillary flow during loss of gas from a core sample, a process which is dependent on molecular volumes for gas fractionation, but not for isotopic enrichments, is probably the second process.

In a recent study of $^{13}C/^{12}C$ ratios in ice-core methane (*5*), Craig *et al.* carried out two experiments of vacuum pumping on 25-g samples of "wafered" ice from 190 m depth in a Dye 3 core. Gas losses relative to a visually unfractured sample were ~46% for O_2, ~44% for Ar, and ~43% for N_2, with resulting $\Delta(O_2/N_2)$ and $\Delta(Ar/N_2)$ values of −64.1 and −8.5 per mil for one sample, and −61.6 and −27.7 per mil for the second. In a later experiment the outer 15% of a cracked ice sample was removed by sublimation in vacuum at −10°C, and $\Delta(O_2/N_2)$ and $\Delta(Ar/N_2)$ values of −43.5 and −19.8 per mil were obtained for the residual gases. Similar values (−32 per mil and −11.4 per mil) were observed by Horibe *et al.* (*1*) on a sample of 20,000-year-old ice. These fractionation effects in gas loss correspond to a ratio of $\Delta(O_2/N_2)$ to $\Delta(Ar/N_2)$ of approximately 2, and we have drawn this vector from the origin in Fig. 3 and from the point of maximum enrichments of O_2 and Ar. Although there is considerable scatter, the majority of points with negative Δ values are approximately aligned with these vectors, including the D-57 samples at the maximum enrichment values. Some of the scatter to large negative $\Delta(Ar/N_2)$ values is the result of errors for Ar, as shown by analyses of six air standards (*3*).

We note three points about the effect of gas losses: (i) these effects have been shown to arise as artifacts of laboratory procedure in fractured samples and may occur when microfractures, almost too small to see, are present; (ii) these losses might also occur during storage of microfractured samples by diffusive loss of gases compressed to high pressures in bubbles; and (iii) the depletion order for major gases is O_2, Ar, and then N_2, so that the heavier gases are removed preferentially, but the heavy isotopes ^{15}N and ^{18}O will always be enriched relative to the light isotopes. This is the case because the isotopic loss rates are independent of molecular volumes and depend only on atomic masses. However, the transport rates for different gases through microfractures will be similar to capillary flow phenomena and thus will be inversely proportional to molecular diameters as well as to mass. The collision diameters for O_2, Ar, and N_2 are 3.467, 3.542, and 3.798×10^{-8} cm (*12*), which is the order of loss rates observed in our pumping experiments. Although still qualitative, these considerations appear to be a plausible explanation of the negative $\Delta(O_2/N_2)$ and $\Delta(Ar/N_2)$ values clustered along the "gas-loss" vector in Fig. 3. Comparison with the experimental effects of gas loss on elemental ratios cited above indicates that these samples have suffered losses of up to ~10% of original gas content during gas extraction by the URI technique or during storage, or both.

A competing process for the positive enrichments of heavy isotopes and gases is simple effusion from partially sintered micropores, in the region just above the firn-ice transition layer. In the simplest case when molecular interactions are neglected, the Δ values are simply proportional to the inverse $M^{1/2}$ ratios and to the amount of gas lost from the pores by effusion (*13*). For this process to be effective the pore openings must be small relative to the molecular mean free paths, but when this is the case the advective velocity necessary for removal of the effusate will have decreased almost to zero (*10*). In Table 1 we compare some of the enrichments expected for the processes of effusion and gravitational settling. We chose $Z = 75$ m and $T = -20$°C, so that $\delta(^{15}N) = 0.35$ per mil for gravitational enrichment, and normalized the effusion enrichment by choosing a 2% loss of gas from the material just undergoing occlusion into nascent ice to provide the same ^{15}N enrichment. The ^{18}O, O_2/N_2, and Ar/N_2 enrichments are similar for the two processes, once the fraction lost is chosen to provide the same ^{15}N enrichment. Lighter gases show more differences, but have no simple atmospherically defined basis for comparison. The Kr/N_2 ratio enrichment differs significantly (as does Xe/N_2), so that careful comparisons with ^{15}N enrichments will provide a definitive choice. However, because the maximum values of these isotopic and gas species enrichments agree well with the values predicted for gravitational separation in the firn, based simply on depth and, to a lesser extent, temperature, the data already in hand are strong evidence for the dominance of the gravitational separation effect (*14*).

The gravitational isotopic enrichments are significant corrections to observed isotopic data for CO_2, CH_4, and O_2 in ice cores. For CO_2 and CH_4 the $^{13}C/^{12}C$ ratio enrichment relative to atmospheric values will be equal to the ~0.3 per mil effect for ^{15}N (Fig. 2): this value is 30% of the observed 1 per mil ^{13}C enrichment in CO_2 in 400-year-old ice (*15*), and 15% of the 2 per mil depletion of ^{13}C in CH_4 in ancient ice (*5*). For atmospheric O_2 the effects are more striking because the maximum enrichment effect for ^{18}O is ~0.6 per mil (2 AMU). Applying this correction to $\delta(^{18}O)$ values for O_2 in 6,100- and 20,000-year-old Camp Century ice (*1*), and noting that mean seawater was enriched in ^{18}O relative to the present value by 0.1 and 1.0 per mil at those times (*16*), we calculate that the ^{18}O enrichment of atmospheric O_2 was 0.4 per mil and 0.6 per mil less relative to mean seawater, rather than significantly greater as indicated by the uncorrected data. These isotopic differences are related to O_2 production and consumption rates which can be evaluated from the ice core data (*1*) if corrected for gravitational effects by analysis of ^{15}N enrichments in the same samples.

Since the classic demonstration by Gibbs (*9*) that substances at thermodynamic equilibrium in a gravitational field should be stratified according to molecular weight, scientists have searched oceans, lakes, and even crystalline rocks for evidence of this effect. The requirement for establishing the Gibbs equilibrium distribution is that vertical mixing occur primarily by molecular diffusion, so that chemical potentials are directly responsible for maintaining the concentration gradients.

Dansgaard (*17*) searched for $H_2{}^{18}O$ enrichment in the deep waters of the Philippine Trench, on the basis of reported isotopic enrichments in Lake Baikal (*18*). Neither region could have yielded a positive result:

convective mixing from heat flow and thermohaline circulation simply destroys the molecular diffusion regime. But in the polar ice caps another effect intervenes: the accumulating firn acts like a giant columnar sieve through which the gravitational enrichment can be maintained by molecular diffusion undisturbed by convective motions. Positive enrichments of the isotopic and gas components that are less than the maximum predicted values probably represent significant variations in accumulation rates that determine the advective efflux of air from the firn back to the atmosphere, as well as with artifacts of analytical procedure when microfractures are present. Thus, 60 years after publication of the canonical theorem of Gibbs, a fluid system at the earth's surface—atmospheric gases in the firn layers of polar ice caps—has provided experimental verification of this effect (*19*).

REFERENCES AND NOTES

1. Y. Horibe, K. Shigehara, C. C. Langway, Jr., *Earth Planet. Sci. Lett.* **73**, 207 (1985).
2. M. Bender *et al.*, *Nature* **318**, 349 (1985).
3. T. A. Sowers, thesis, University of Rhode Island, Kingston (1987); T. Sowers, M. Bender, D. Raynaud, *J. Geophys. Res.*, in press.
4. H. Friedli *et al.*, *Nature* **324**, 237 (1986).
5. H. Craig, C. C. Chou, J. A. Welhan, C. M. Stevens, A. Engelkemeir, *Science* **242**, 1535 (1988).
6. The δ values, in per mil, $= 10^3 \cdot [(R/T_A) - 1]$ where R is the $^{18}O/^{16}O$ or $^{15}N/^{14}N$ ratio and R_A refers to the atmospheric ratio. We use δ for isotopic enrichments and Δ for enrichments of the molecular ratios O_2/N_2 and Ar/N_2.
7. At SIO gases were extracted from ~257-g ice samples by vacuum melting and cycled over hot carbon to convert O_2 to CO_2 as in (*1*). The remaining N_2-Ar fraction was input through I_2O_5 reagent (which totally removes CO) to our mass spectrometer for ^{15}N measurements. All samples were interspersed with standards containing the atmospheric N_2/Ar ratio. The methods used in the URI work are described in (*3*).
8. W. S. B. Paterson, *The Physics of Glaciers* (Pergamon Press, Oxford, ed. 2, 1981).
9. J. W. Gibbs, *Collected Works*, vol. 1, *Thermodynamics* (Yale Univ. Press, New Haven, 1928).
10. The firn density curve (7) was fit with an exponential from which the upward flux of air at any depth Z can be calculated as $(1/\rho_z - 1/\rho_t)$ times the ice accumulation rate, where ρ_t is the final density (0.83) at the firn to ice transition. The ratio of diffusive to advective gas fluxes can then be calculated approximately from the exponential concentration gradient: for N_2 this ratio varies from 0.16 at the surface, to 1 at $Z = 40$ m, to 24 at $Z = 68$ m, and is infinite at the transition layer. This ratio, and thus the accumulation rate, may be the controlling effect on scaling the effective isotopic enrichment relative to the calculated maximum value for zero advection. The advection velocity of gas varies from ~50 cm/year at the surface, to 1 cm/year at 65 m depth, and to 0 at the firn-ice interface.
11. D. Raynaud and J. M. Barnola, *Nature* **315**, 309 (1985).
12. R. C. Reid and T. K. Sherwood, *The Properties of Gases and Liquids* (McGraw-Hill, New York, ed. 2, 1966). The collision diameters are the Lennard-Jones potential values derived from viscosity data.
13. The effusion equation for Δ (or δ) is, in simplest form (no molecular interactions):

$$\Delta \sim [(M/M_i)^{0.5} - 1] \cdot 10^3 \cdot F_L \quad (3)$$

where F_L is the fraction of gas lost in the actual fractionating process. For ^{15}N the "single-stage enrichment" term is 17.3 per mil, which with a 2% loss of N_2 would give $\Delta = 0.35$ per mil.
14. In Eq. 1, it is assumed that gases in an element of firn continuously readjust to the time-independent equilibrium state as each element advects from the surface down to the firn-ice transition zone. The e-folding time for molecular diffusion over half the firn depth is $\sim(Z/2)^2/D$ (D is the diffusion coefficient in air), which is of the order of 1 year, during which time a firn element moves downward by ~0.5 to 0.02 m, so that this assumption is approximately true. A complete description of the gases in the firn column requires solutions of the diffusion equations in a porous medium with a moving boundary in a gravitational field, temperature gradients, coupling terms between diffusion coefficients of major components, vertical variation in the upward advection rate of gases (*10*), and the transient mixing effects of barometric pressure waves in the column. The barometric effects have a time scale of the order of weeks to months at the surface and are rapidly attenuated with depth by the decreasing porosity and increased resistance to gas flow, so that all these effects, the details of which are beyond the scope of this first paper, are expected to be of second order or less in importance.
15. H. Friedli, E. Moor, H. Oeschger, U. Siegenthaler, B. Stauffer, *Geophys. Res. Lett.* **11**, 1145 (1984).
16. L. D. Labeyrie, J. C. Duplessy, P. L. Blanc, *Nature* **327**, 477 (1987).
17. W. Dansgaard, *Deep Sea Res.* **6**, 346 (1960).
18. J. Mendelejev, *Dokl. Akad. Nauk SSSR* **3**, 105 (1935).
19. After completion of this paper and presentation as an A. L. Day lecture at Yale University, we learned that J. Schwander has discussed the possibility of gravitational effects on gas chemistry in firn [in *Proceeding of the Dahlen Workshop on the Environmental Record of Glaciers*, H. Oeschger and C. C. Langway, Jr., Eds. (Wiley, New York, in press)].

20. We thank D. Burtner and C. Nilson at SIO for dedicated assistance in the laboratory, M. Bender at URI for discussion, and V. K. Craig for the manuscript. H.C. thanks H. Ramberg for exciting his initial interest in gravitational thermodynamics. Work at SIO was supported by NSF grants DPP85-21486 and DPP87-22718; work at URI was supported by grant OCE85-01197 (M. Bender).

11 October 1988; accepted 9 November 1988

Restoration of Torque in Defective Flagellar Motors

DAVID F. BLAIR AND HOWARD C. BERG

Paralyzed motors of *motA* and *motB* point and deletion mutants of *Escherichia coli* were repaired by synthesis of wild-type protein. As found earlier with a point mutant of *motB*, torque was restored in a series of equally spaced steps. The size of the steps was the same for both MotA and MotB. Motors with one torque generator spent more time spinning counterclockwise than did motors with two or more generators. In deletion mutants, stepwise decreases in torque, rare in point mutants, were common. Several cells stopped accelerating after eight steps, suggesting that the maximum complement of torque generators is eight. Each generator appears to contain both MotA and MotB.

CELLS OF *Escherichia coli* AND MANY other motile bacteria swim by rotating helical flagellar filaments (*1, 2*). Each filament is driven at its base by a motor powered by the transmembrane proton gradient (*3*). The motor is only about 20 nm in diameter but is moderately complex, containing about 20 different polypeptides (*4*). Basal structures have been purified (*5, 6*) and shown by electron microscopy to consist of four rings (two in Gram-positive bacteria) mounted on a rod (*6, 7*). These basal structures are missing several proteins essential for torque generation (*8*), including MotA and MotB, which are both found in the cytoplasmic membrane (*9*). Mutants defective in MotA or MotB are paralyzed; their motors do not generate torque, even though the basal structures appear normal (*9, 10*). By inducing transcription of a wild-type *motB* gene carried on a plasmid in tethered cells of a *motB* missense mutant, Block and Berg (*11*) showed that restoration of torque takes place in a series of equal steps, indicating that MotB is a component in each of several independent torque generators. Here, we extend these studies to MotA as well as MotB, by use of deletion as well as missense mutants.

Cells of *motA* or *motB* strains were transformed with plasmids that carry *motA* or *motB* fused to the lactose promoter and $lacI^Q$ (an allele that overexpresses the structural gene for the *lac* repressor (*12*) (Table 1).

Table 1. Strains and plasmids.

Strain or plasmid	Relevant genotype
RP437	Wild type for motility and chemotaxis
MS5037	*motA*
RP3087	*motB 580*
RP6666	Δ*motA*
BL-19	Δ*motB1*
RP6894	Δ*motA*Δ*motB*
pDFB27	p*ara-motA*$^+$*motB*$^+$, *araC*$^+$, *Ap*^{R}
pDFB28	p*lac-motB*$^+$, *lacI*^{Q}, *Ap*^{R}
pDFB29	p*ara-motA*$^+$, *araC*$^+$, *Ap*^{R}
pDFB36	p*lac-motA*$^+$, *lacI*^{Q}, *Ap*^{R}
pSYC62	p*mocha-motB*$^+$, *Cm*^{R}

Department of Cellular and Developmental Biology, Harvard University, Cambridge, MA 02138, and the Rowland Institute for Science, Cambridge, MA 02142.